KUE

1994 KRAFLA UNDERSHOOTING EXPERIMENT

Submitted by
William Menke, Bryndis Brandsdottir, and Pall Einarsson
Lamont-Doherty Earth Observatory
Science Institute, University of Iceland

PASSCAL Data Report 95-002

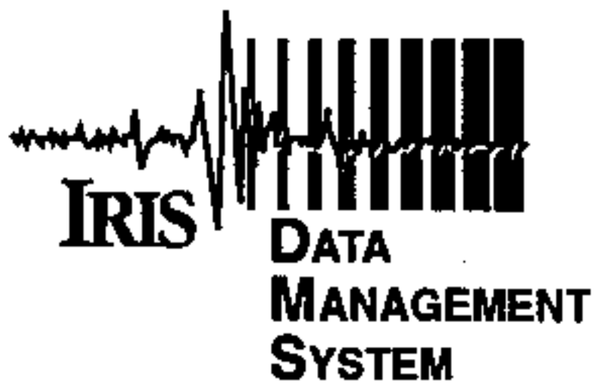

Distributed by

Incorporated Research Institutions for Seismology
Data Management Center
1408 NE 45th Street
2nd Floor
Seattle, Washington 98105

Technical Report

CRUSTAL STRUCTURE OF THE KRAFLA CENTRAL VOLCANO IN THE NORTHERN VOLCANIC ZONE OF ICELAND AS DETERMINED THROUGH SEISMIC OBSERVATIONS

Bryndís Brandsdóttir[1], William Menke[2], Páll Einarsson[1], Robert White[3], Robert Staples[3], and members of the Faeroes-Iceland Ridge Experiment (FIRE).

[1]*Science Institute, University of Iceland, Dunhaga 5, IS-107 Reykjavík, Iceland; fax: 354-1-28911; E-mail: bryndis@raunvis.hi.is, palli@raunvis.hi.is*

[2]*Lamont-Doherty Earth Observatory and Department of Geological Sciences, Columbia University, Rt. 9W Palisades, NY10964, USA fax: 914-365-8150; E-mail: menke@lamont.ldeo.columbia.edu*

[3]*Department of Earth Sciences, University of Cambridge, Bullard Laboratories, Madingley Road, Cambridge CB3 OEZ fax: 441-223-60779; E-mail: rwhite@esc.cam.ac.uk, staples@esc.cam.ac.uk*

Science Institute, University of Iceland
New York, July 1995.

Internal Report RH-95-05

1 Introduction

Iceland has been built by hot spot volcanism at a slow spreading ridge. The volcanism is driven by mantle plume processes and rifting at the divergent mid-Atlantic plate boundary. The average half-spreading rate is 10 mm/year in the Iceland region. The interaction between the westward drifting plate boundary and the stationary hot spot has induced eastward jumps of the plate boundary, resulting in the present expression of the Neovolcanic zones in Iceland (Figure 1). The rift zone in northern Iceland (the Northern Volcanic Zone) became active following an eastward jump 6-7 m.y. ago [Sæmundsson, 1979].

Volcanism in Iceland is confined to volcanic systems which, in many ways, correspond to the spreading segments of the mid-Atlantic ridge. Each volcanic system consists of a central volcano, where the productivity is highest, and a transecting fissure swarm. Geological, K/Ar dating and paleomagnetic studies indicate that each central volcano has a life span of 0.3-1.0 M years, after which the center of activity shifts to a new location along the plate boundary [Sæmundsson, pers. comm. 1995]. The central volcanoes are circular in outline and 20-40 km in diameter. They are spaced 20-70 km apart along the plate boundary (Figure 1). Many have a caldera, acidic volcanism and a high-temperature geothermal system associated with them [Sæmundsson, 1978; Einarsson and Sæmundsson, 1987].

1.1 The crustal structure of Iceland

The first seismic refraction experiment in Iceland, a 250 km long profile, revealed P-velocities of 3.69-6.71 km/s in the uppermost 17.8 km, increasing to 7.38 km/s at a depth of 18-28 km [Båth, 1960]. Båth divided the crust into three layers and determined its thickness to be 27.8 km. He pointed out that the compressional velocity of 6.71 km/s (layer 2) agreed well with crustal velocities in the N-Atlantic. However, velocities in his third layer corresponded to those of the deeper layer of the mid-Atlantic ridge, which Ewing and Ewing [1959] considered to be made up of a mixture of oceanic crust and mantle and which are now thought to be gabbroic cumulates.

Tryggvason [1962] uses surface wave dispersion analysis to divide the Icelandic crust into a 10-km-thick, two-layer stack overlying a halfspace with a compressional velocity of 7.4 km/s and a shear wave velocity of 4.3 km/s. He concludes that the halfspace represents anomalously slow "mantle". His velocity structure is in fact similar to the earlier refraction studies, but he gives a significantly different interpretation of material at 10 km depth and deeper, calling it "mantle" rather than "Oceanic layer 3A". Measurements of P wave traveltimes from teleseisms gave anomalously low compressional velocities (7.4 km/s) in a 234±14 km thick region

under Iceland (assuming a crustal thickness of 17 km under Reykjavík) [Tryggvason, 1964]. Francis [1969], on the basis of high V_p/V_s ratios, found the low-velocity region to be 300 km wide along the mid-Atlantic ridge crossing Iceland, and that it extended down to 250 km depth. Both claimed that P-velocities of 7.4 km/s belong to the mantle.

This difference in interpretation persists in the literature. For instance, the "mantle" interpretation is used by Pálmason [1963; 1971], who divides Iceland into 5 layers, numbered 0-4, with layer 4 (V_p=7.2 km/s; 8-16 km depth) being anomalously slow "mantle". Later surveys [Zverev et al., 1976; Angenheister et al., 1980; Gebrande et al., 1980; Bjarnason et al., 1993] as well as reinterpretations of Pálmason's data [Flóvenz and Gunnarsson, 1991] all confirmed earlier velocity measurements (P-velocities of 7.0-7.4 km/s at depths of 10-30 km), but were interpreted in contradicting ways. Some researchers interpreted P-velocities higher than 7.0 km/s as anomalously slow "mantle" [Pálmason, 1963, 1971; Angenheister et al., 1980; Gebrande et al., 1980; Flóvenz and Gunnarsson, 1991], while others [Zverev et al., 1976; Bjarnason et al., 1993] interpretated them as lower crust. However, Angenheister et al., [1980], noting discontinuous second arrivals from the RRISP shot D, mention an alternative interpretation of the data, i.e., that the second P arrival, which has an apparent velocity of 7.8 km/s [Gebrande et al., 1980], may indicate a crustal thickness of 30 km under Iceland. In our opinion, the later arrival from shot D is a clear Moho reflected phase (P_mP) and is evidence that the crustal thickness is close to 30 km under the Neovolcanic zone, in central Iceland.

The question of the depth to mantle is, in principle, equivalent to the question of the thickness of the crust. Yet the two questions have had a rather decoupled history in Iceland, owing to the somewhat different analytical approaches to the underlying seismic datasets. The idea of crustal thickness is most sensible when a sharp increase in velocity, or Moho, marks the boundary between crust and mantle. Hence, crustal thickness measurements are to some degree related to the detection of the Moho-reflected phase, P_mP. Furthermore, the controversy regarding the proper interpretation of Pálmason's layer 4 spawned a related controversy regarding whether or not reflected phases occur in Iceland and, if they do, whether they really represent reflections from the Moho, as contrasted to some deeper interface within the mantle [Gudmundsson, 1994; Bjarnason et al., 1994].

Zverev et al. [1976] used data from the North-Atlantic Seismic Project (NASP) to analyse the crustal thickness below the Iceland-Faeroe-Shetland region, and data from two stations in E-Iceland and one station in the Neovolcanic zone to infer a crustal thickness of 40-60 km beneath Iceland. Zverev et al. [1976] claimed that crustal velocities below 8 km/s belonged to the crust. They did not detect a Moho reflector, but they observed a significant increase in crustal thickness towards the Neovolcanic zone. The 7-km/s isovelocity surface dips from 15 km depth in

Reydarfjördur, at the eastern coast, to 30 km at station DU5, in the Neovolcanic zone.

Bott and Gunnarsson [1980], analysing the same NASP-data, detected Moho arrivals at about 23 km depth (time-term = 1.8) below the eastern coast and at about 27 km (time-term = 2.3s) depth at station DU5, in the Neovolcanic zone. The Moho refractor has a phase velocity of 7.8 km/s. Seismic refraction data from SW-Iceland revealed a clear wide-angle reflection from a reflector at a depth of 20-24 km, which Bjarnason et al. (1993) interpret as Moho. This reflector is underlain by a low-velocity mantle, as upper mantle compressional velocities are 7.6-7.7 km/s at the Moho. The "lower crust" interpretation of layer 4 by Zverev et al. (1976), based on NASP-data, was largely ignored in the subsequent literature.

The structural model of Iceland that emerged in the late 1970's and early 1980's was that of a relatively thin, 10-to-15-km-thick, crust overlying a very hot and partially molten mantle. It was based on seismic [Tryggvason, 1962; Gebrande et al., 1980] and magnetotelluric data [Beblo and Björnsson, 1980], and supported by the linear extrapolation of temperature gradients in shallow geothermal boreholes [Pálmason, 1971; Pálmason and Sæmundsson, 1974, 1979]. The crust was thinnest under the Neovolcanic zone. An approximately 5-km-thick, high-electrical conductivity layer at 10-20 km depth under NE-Iceland, revealed by magnetotelluric soundings, has been interpretated as the region of partial melt from which shallow crustal magma chambers derive their melt [Beblo and Björnsson, 1980].

Shear wave measurements are particularly relevant to the question of the presense of melt. Shear waves cannot propagate through a completely molten layer and are attenuated very rapidly in regions of partial melt. For instance, using Mavko's [1980] estimate of the shear wave quality factor, Q_s=2, for a 3% partial melt, the amplitude of a 10 Hz shear wave would be reduced by an order of magnitude in only 0.5 km. At hot (>800°C) but sub-solidus temperatures, shear wave attenuation should also be high (Q_s<20) and the ratios of compressional to shear wave velocity, V_p/V_s, should be considerably higher than the 1.73 expected for a normal solid, in the range of 1.9-2.0.

Regional shear waves, with turning points in the mid- to lower crust are observed in Iceland. Tryggvason and Båth [1961], Tryggvason [1962], Pálmason [1971], and Gebrande et al. [1980] all identify shear-waves in their data, although they are usually more prominent on raypaths outside the Neovolcanic zone. Sanford and Einarsson [1982] report that shear waves from earthquakes in NE-Iceland propagate down to at least 10 km depth in the Northern Volcanic Zone, precluding the existence of large scale magma bodies at shallow depths. Pálmason [1963] reported V_p/V_s ratios of 1.79, 1.85, and 1.80 for crustal layers 1, 2 and 3, respectively, in northern and eastern Iceland. These values are somewhat higher than in western (1.72-1.75) [Tryggvason, 1962] and southwestern Iceland (1.74-1.78) [Menke et al., 1994].

Gebrande et al. [1980] present two "mostly" horizontal-component record sections that display shear waves. One record section (shotpoint E, their Figure 7), a shot in Vopnafjördur observed on a line extending to the southwest, has V_p/V_s=1.76 out to a range of 120-140 km (Figure 2). According to those authors, it "becomes progressively late" at greater ranges, with V_p/V_s increasing to 2.2. A somewhat different behaviour is exhibited by the other record section (shotpoint G, their Figure 8), from a shot north of Heimaey observed on the RRISP profile II, extending to the east-northeast (Figure 2). The S-wave is clearly observed out to ranges of 165 km, after which it disappears. It is systematically delayed by about 1 s from what would be predicted by V_p/V_s=1.76. Thus, it has V_p/V_s ratios in the 1.9-2.1 range.

Gebrande et al.'s [1980] shear wave record sections are important because they demonstrate the very unusual propagation of S waves in the Icelandic crust. However, our interpretation of these data, especially in light of our experience in northern Iceland, is completely different than theirs: First, the disappearance (or delay) of the S wave at ranges greater than 120-140 and 165 km corresponds to points where the RRISP-profiles cross active volcanic systems (Askja, Bárdarbunga, and Tungnafellsjökull for Shot E, and Öræfajökull for Shot G). Therefore, we believe that the disappearance is due to the shallow structure in and near these volcanoes and not to melt in the deep crust.

This S wave attenuation may be similar to the attenuation that [Einarsson, 1978] identifies in the shallow (3-7 km) crust beneath Krafla and which is associated with the shallow magma chamber of that volcano. The magma chamber itself completely shadows S waves. Our data shows that the magma chamber is surrounded by a larger region of elevated temperatures that is highly attenuating (Q_s=10), as well. Rays that pass through this shallow attenuating region will have low shear wave amplitudes. Furthermore, we believe that the phase from Shot E, identified by the authors as a 'delayed S' phase (i.e., for ranges greater than 140 km), is in fact a $S_mS$or a S_{ref}phase. Both S and S_mS(or S_{ref}) phases are clearly present at ranges of 100-140 km, where the profile runs along the eastern border of the Askja central volcano. Indeed, as we will discuss further below, the similarity between the RRISP Profile E and several of our N-Iceland profiles, in which P and S waves and their reflected analogs are all clearly present, is startling. In our new interpretation, the RRISP profile E does not require anomalously slow lower-crustal shear wave velocities.

RRISP Profile G, which has a 'delayed' S wave out to 165 km, has also been used to argue for anomalously slow lower-crustal shear wave velocities. However, the constant delay of the S-wave is not consistent with this interpretation, but is rather diagnostic of a source static anomaly, or very complicated propagations paths (most of the raypaths cross Katla volcano), or possibly some combination of source location and timing errors. A close examination of the P waves for this profile indicates that seismograms from the two component shots (G1 and G2) are offset

by 0.5s. Furthermore, readings from the Iceland station network [Einarsson, 1979] for this shot, at stations adjacent to the RRISP profile, are systematically advanced by about 0.5 s with respect to the RRISP readings (Figure 3). We have not been able to determine the explanation for these differences. However, they are further indications of the problems of measuring traveltimes from this record section. While there is some kind of anomaly present in the G profile, we do not feel that it can be explained by anomalously slow shear wave propagation. Furthermore, the RRISP E profile does not require anomalously slow lower-crustal shear wave velocities either.

Recent shear wave attenuation studies from local earthquakes in S-Iceland indicate that the lower crust has a relatively high quality factor (Q_s=200-600) and therefore cannot contain partial melt [Menke and Levin, 1994; Menke et al., 1995]. Indeed, these authors argue that the high Q's imply temperatures significantly below the solidus, with 900°C as an upper limit, in the lower crust in Iceland. Consequently, these studies support the interpretion that the 10-20 km depth interval is lower crust, similar in properties to Oceanic Layer 3A. The presence of thicker crust (>20 km) above the Iceland hot spot is more consistent with geochemical upper mantle melting models [McKenzie, 1984; Klein and Langmuir, 1987] and with rare-earth isotopic inversions [White et al., 1992]. Furthermore, a new thermal model of Iceland has been developed that incorporates the processes of plate tectonic spreading, melt generation in the mantle, and cooling of the lithosphere [Menke and Sparks, 1995]. It is able to explain the observed heatflow, shear wave quality factors, and maximum depth of earthquake hypocenters by modelling a 20-km-thick, sub-solidus crust.

Reviewing older data, we cannot find any seismic measurements that support the thin, hot crust model. For instance, Tryggvason's [1962] original data do not support this interpretation, because the V_p/V_s ratio of the "mantle" halfspace is 1.72, which is not diagnostic of melt. Indeed, it is lower than the 1.74-1.75 he reports for the crust. Bott and Gunnarsson [1980] identify Moho arrivals under Iceland in the NASP-data. Gebrande et al.'s [1980] high V_p/V_s is more likely caused by local crustal anomalies associated with central volcanoes than by partially molten ultrabasic material at depth. In Iceland as elsewhere, compressional velocites of 7.0-7.4 km/s should be attributed to the crust. Thereby the alternate interpretation of the RRISP-data [Angenheister et al., 1980] shows that the thickness of the Icelandic crust is 30 km, or more.

In our opinion, the hypothesis of a thick, sub-solidus crust is supported by more data than the alternate, partially molten mantle hypothesis. Nevertheless, many important questions remain unresolved: It is uncertain whether or not the material below the Moho is normal, peridotitic mantle. Certainly its seismic velocity is anomalously low (7.6-7.7 km/s), an effect which might be due to temperature or, analogous to Caress et al.'s [1995] interpretation of the Marquesas hotspot, to

underplating by crustal rocks. Just how the magnetotelluric data can be explained within the context of a sub-solidus crust remains a puzzle. The high electrical condictivities cannot be due to partial melt, and therefore must be due to some other physical or chemical change occuring at mid-crustal depths. Finally, how the crust forms at the volcanic zones and how it subsequently evolves over geologic time need to be addressed. We will later present new data which bear on these questions.

In the discussion below, we will adhere to Pálmason's numbering scheme for the gross crustal structure, which we preface with a 'P' so as to distinguish it from the oceanic nomenclature. Layers P-0 (porous lavas, V_p=2.75 km/s) and P-1 (flood basalt, V_p=4.14 km/s) are analogous to Oceanic Layer 2a. Layer P-2 (V_p=5.08 km/s; less porous basalt) is analogous to Oceanic Layer 2b. Layer P-3 (V_p=6.5 km/s; metamorphic facies of basaltic rocks) is analogous to Oceanic Layer 3A. Layer P-4 (V_p=7.2 km/s; formerly interpreted as mantle) is analogous to Oceanic Layer 3B (gabbros and metagabbros).

1.2 The Northern Volcanic Zone

The Northern Volcanic Zone (NVZ) is composed of seven NNE-SSW elongated volcanic systems arranged *en echelon* along the plate boundary. They are: Theistareykir, Krafla, Fremri-Námur, Askja, Kverkfjöll, Bárdarbunga, and Tungnafellsjökull. The plate boundary is about 50 km wide in northern Iceland, but broadens to 80 km in central Iceland, where the Kverkfjöll, Bárdarbunga, and Tungnafellsjökull volcanic systems overlap at the junction of the NVZ with a cluster of volcanic systems in central Iceland (Figure 1). Fissure swarms, characterized by rifting structures such as crater rows, normal faults and open fissures, transect the central volcanoes at an azimuth perpendicular to the regional spreading direction.

Variations in petrology and topography of the NVZ represent the different evolutionary stages of individual volcanic systems. The Krafla, Askja, Kverkfjöll, Bárdarbunga, and Tungnafellsjökull central volcanoes, with developed calderas, represent the most mature volcanic systems [Sæmundsson, 1982]. Aeromagnetic surveys show strong positive magnetic fields surrounding pronounced, equidimensional negative anomalies over the Krafla and Askja central volcanoes, whereas strong elliptical and arcuate positive anomalies occur over the Kverkfjöll and Bárdarbunga central volcanoes [Jónsson and Kristjánsson, 1991]. The positive anomalies are most likely related to shallow intrusives with high magnetization. The negative anomalies over the Askja and Krafla-Námafjall areas are caused by local hydrothermal alteration of young basalts. However, more detailed data are needed about the petrology and the seismic structure of the NVZ before we can fully understand the magnetic anomalies.

The petrogenesis of the NVZ is reflected in the chemical composition of its

tholeiitic rock suites. The rift zone volcanoes are fundamentally basaltic in composition, with relatively small volumes of more evolved rocks [Sæmundsson, 1978; Grönvold, pers. comm., 1995]. Petrochemical and isotopic data indicate that the rhyolites are formed by remelting of hydrated crust [O'Nions and Grönvold, 1973; Sigmarsson et al., 1991; Jónasson, 1994] and that crustal assimilation plays a significant role in the petrogenesis of the most differentiated rocks as well as for the rift-zone tholeiites [Óskarsson et al., 1982; Nicholson et al., 1991]. In order to explain these processes, we have to evoke crustal magma chambers large enough to remelt the adjacent crust and produce silicic magmas. It is thus evident that crustal magma chambers must play an important role in the crustal genesis of Iceland. Based on the map distribution of silicic rocks [Jóhannesson and Sæmundsson, 1989], one can easily point out the central volcanoes which must have, at some point in their history, hosted crustal magma chambers. The Krafla central volcano is one of them.

Volcanic activity in the Northern Volcanic Zone during the last three centuries has been confined to the Krafla and Askja volcanic systems. During this time three rifting episodes occurred in the Askja system (1874-1876, 1921-1933, and 1961-1962) and two in the Krafla volcanic system (1724-1729 and 1974-1984). The eruptive activity of these volcanic systems indicates that the general structure of magmatism associated with them consists of the episodic accumulation of magma in small, shallow, crustal magma chambers, followed by the migration of this magma away from the magma chamber into dike systems parallel to the ridge [Björnsson et al., 1977; Sigurdsson and Sparks, 1978; Einarsson, 1991a,b; Sæmundsson, 1991; Brandsdóttir, 1993]. The recent rifting activity in the Krafla volcanic system offered an unique opportunity to study crustal rifting and magmatism associated with a shallow crustal magma chamber situated on a rift axis [Björnsson et al., 1977; Einarsson, 1978; Brandsdóttir and Einarsson, 1979; Einarsson and Brandsdóttir, 1980; Tryggvason, 1980, 1984, 1986; Grönvold, 1988; Björnsson, 1985; Einarsson, 1991a,b; Brandsdóttir and Menke, 1992; Arnott and Foulger 1994a,b].

1.3 The Krafla volcanic system

The Krafla volcanic system is made up of the Krafla central volcano and a transecting fissure swarm, and it corresponds in many ways to a spreading segment on an oceanic ridge. The central volcano is a major eruptive center which, based on geological mapping, K/Ar dating, and paleomagnetic studies, is less than 500,000 years old [Sæmundsson, pers. comm., 1995]. The Krafla central volcano is approximately 21 km long by 17 km wide, and encloses a 10 km by 7 km caldera that was formed during the last interglacial period 100,000 years ago; it has since been filled with younger hyaloclastites and basaltic lavas [Björnsson et al., 1977; Sæmundsson,

1978, 1982; 1991]. The central volcano has a broad, relatively flat terrain (ranging from 300 to 500 m in elevation) made up of alternating basaltic lava and hyaloclastite sequences [Ármannson et al., 1987]. Interglacial hyaloclastic table mountains and rhyolitic ridges rise up to 900 m elevation. Two main phases of rhyolite volcanism have been identified in the Krafla central volcano, related to the formation of the Krafla caldera [Sæmundsson, 1982; Calderone et al., 1990]. Three rhyolitic ridges situated 2-5 km outside the present caldera rim which were formed during the last glacial period are most likely related to the emplacement of a ring dike [Jónasson, 1994].

The Krafla central volcano is transected by a fissure swarm, approximately 100 km long, striking NNE-SSW. There is a variation in chemical composition of the Krafla tholeiites between the caldera and the transecting fissure swarm. The fissure swarm tholeiites are mostly olivine normative, whereas quartz normative tholeiites are dominant within the Krafla caldera [Grönvold, 1984, 1988; Ármannsson et al., 1987]. On the basis of this chemical difference, Einarsson [1991b] suggested that the more primitive olivine tholeiites were laterally injected into the Krafla fault swarm from the lower levels of the Krafla magma chamber while the quartz-normative tholeiites, which erupted within the caldera, had resided longer at the upper levels of the magma chamber.

Three high-temperature geothermal areas exist within the Krafla central volcano. Two are located approximately 5 km south of the Krafla caldera. They are: Bjarnarflag and Námaskard-Hverarönd. The third, the NW-SE aligned, 15 km^2, Krafla-Leirhnúkur geothermal field, is located inside the Krafla caldera. The eastern part of the Krafla-Leirhnúkur geothermal field is presently harvested by the Krafla power plant, which started operation in 1978. Ármannsson et al. [1987] describe the subsurface lithology and tectonics of the Krafla-Leirhnúkur geothermal field, based on 24 borehole sections. The subsurface formations can be divided into two major sections which most likely represent the overall crustal structure of the Krafla caldera: an upper, extrusive section; and a lower, intrusive section. Each formation is about 1000 m thick. The upper section consists of postglacial lava formations overlying hyaloclastites and interglacial lavas. The lower section consists mainly of basaltic and doleritic intrusives grading down to gabbros at 2000-2200 m depth underneath the easternmost part of the field. Acid intrusions are most abundant above the gabbros, where the hyaloclastite/lava section is underlain by a 100-150 m thick acidic sill at 300-450 m depth. It engulfs a small basaltic sill along with some smaller, deeper-seated sills. The acidic intrusives are most likely derived from the gabbros at 2000 m depth.

A microearthquake study around the geothermal areas of Iceland during the summers of 1967 and 1968 [Ward and Björnsson, 1971] revealed a surprisingly high microearthquake activity in the Krafla region. During the summer of 1967, a

daily average of 191 earthquakes (S-P$\leq$2.5s) was recorded, but the activity dropped to 1.2 events per day (with an average S-P time of 0.4s) in 1968. At the same time, no earthquakes were recorded in the fissure swarms north (Gjástykki) and south (at the southern end of lake Mývatn) of the Krafla central volcano. Ward and Björnsson [1971] suggest that the high activity in 1967 could possibly have been related to an earthquake of magnitude 3-4 that occurred in the Krafla caldera a few days before their deployment. People living 10-20 km from the Krafla region felt this earthquake. Although most of the seismicity in the Neovolcanic zones is confined to high-temperature geothermal areas within the central volcanoes, an earthquake swarm of the same intensity as recorded in the Krafla region in 1967 is highly unusual. Seismic activity of this intensity was not observed again in the Krafla region prior to the Krafla rifting episode. Therefore, the most logical explanation of the 1967 swarm is that the Krafla magma chamber had already started inflating in the summer of 1967 and that the inflation subsequently ceased until 1974.

Permanent seismic stations were not installed in northeastern Iceland until 1974 and 1975. Therefore, little is known about the local microseismic activity prior to the 1974-1985 Krafla rifting episode. The first permanent seismometer was installed in the Krafla region in July 1975. This station, Reynihlíd, which is situated 10 km southwest from the center of the caldera, was installed after new stations at Húsavík and Grímsstadir, 40 km NW and 30 km E of Krafla, had indicated an unusally high level of activity within the Krafla caldera. At that time, 10-15 earthquakes originated within the Krafla caldera per day. The seismic activity increased in the fall of 1975 and by then people living 10-20 km away from the volcano had begun feeling the earthquakes [Einarsson, 1991b]. Scientists speculated about the possible causes of the increased seismicity, but an eruption on December 20th, 1975, answered their questions. The Krafla rifting episode had begun.

The 1974-1985 rifting activity in the Krafla volcanic system consisted of long periods of inflation, during which magma accumulated at a shallow depth within the caldera region, and short deflation periods when the magma was laterally intruded into the associated fissure swarm or was erupted at the surface. The inflation/deflation cycles were regulated by increasing/decreasing pressure in the Krafla magma chamber and by tectonic stress at the diverging plate boundary. The inflation periods were characterized by intense seismicity in the region above the Krafla magma chamber, whereas migrating earthquake activity accompanyied the lateral dike intrusions and rifting in the Krafla fissure swarm. During 1974-1985, twenty inflation/deflation cycles took place in the Krafla volcanic system, activating most of the 100-km-long fissure swarm. Nine of these deflations were accompanied by basaltic fissure eruptions. The last deflation/eruption event took place in September 1984 after which the magma chamber inflated normally during the next 3 months. The inflation halted in early 1985. Brief periods of inflation occurred in 1986-1989,

during which increased seismic activity in the uppermost 3 km around the center of inflation was generated by the increasing differential stress in the region above the magma chamber. Currently, the seismic activity (less than 1 microearthquake per day) is mostly confined to the Krafla and Bjarnarflag geothermal regions.

Einarsson [1978] used local earthquakes recorded during an inflation period in order to delineate two regions of shear wave attenuation. He inferred that there is a shallow crustal magma reservoir at a depth of approximately 3 km, near the center of inflation in the caldera. This magma chamber is smaller than the caldera, about 2 km by 7 km, with the long axis oriented E-W and divided near its top. The southern boundary of the magma chamber is better defined than the northern boundary. Its maximum depth of roughly 7 km is not well-constrained. Brandsdóttir and Menke [1992] performed waveform studies on earthquakes which originated within the Krafla caldera during a brief inflation period in July 1988 in order to study the thickness of the magma chamber. They identified reflections from beneath the magma chamber which indicated that it was less than 1 km thick in the central-northern part of the caldera, but they could not constrain its lateral dimensions. Geodetic measurements support the existence of a shallow magma chamber at a depth of 3 km within the caldera and have been used to argue for the existence of multiple magma reservoirs at depth [Tryggvason, 1986].

Arnott and Foulger [1994a] used local earthquakes and artificial sources recorded at a local array of seismic stations to construct a coarse 3-D velocity model for the shallow structure of the Krafla central volcano. Limited depth penetration of rays and deteriorating resolution with depth precluded the detection of the magma chamber, but high velocity bodies were detected around the rim of the Krafla caldera at shallow depth (<3 km). These were interpreted as crystalline intrusives. Unfortunately, Arnott and Foulger's [1994a] model of the upper crustal structure in the Krafla caldera is seriously flawed. We believe that the high velocity bodies in their model are only artifacts of the inversion process caused by a tradeoff between velocity and earthquake source parameters. The refraction data that we present below demonstrates that the shallow seismic structure of the Krafla caldera is relatively flat lying, consistent with the borehole petrologic data.

The year 1994 marked the 270th anniversary of the Mývatn Fires and the 20th anniversary of the Krafla Fires, the two most recent rifting episodes in the Krafla volcanic system. Last year was also the year of the Faeroes-Iceland Ridge Experiment (FIRE), during which we carried out the first seismic undershooting experiment on the Krafla central volcano. The FIRE data, which is currently being analysed at the University of Cambridge, will provide new results on the crustal structure along the transect (from the Faeroes, via Eastern Iceland, into Krafla). These data document the interaction of the Iceland mantle plume with the N-Atlantic spreading centre from the time of initial continental breakup to the present day. The Krafla

undershooting experiment was aimed at mapping the seismic structure of the Krafla central volcano and its immediate vicinity in order to further our understanding of the precesses of melt extraction from the uppermost mantle and its emplacement within the crust at a slow spreading ridge. The experiment targeted the lower part of the Krafla magma chamber and the crust-mantle boundary beneath the Neovolcanic zone.

By determining the crustal thickness within and adjacent to the Neovolcanic zone, we can finally distinguish between the two controversial crustal models of Iceland. Our data also constrain the thickness and volume of the Krafla magma chamber and the temperature structure of the Icelandic crust.

2 Experiment Configuration

This report combines data from three different seismic surveys: The 1991 Tjörnes Fracture Zone (TFZ) experiment, the 1993 Krafla reflection/refraction survey, and the 1994 Krafla Undershooting Experiment, which was a part of the Faeroes-Iceland Ridge (FIRE) experiment.

2.1 The 1994 FIRE experiment

The Faeroes-Iceland Ridge Experiment (FIRE) was carried out in July-August 1994 by scientists from the Universities of Cambridge and Leicester in England, the University of Iceland (Reykjavík), Columbia University (New York), and the Danish Geological Survey (Copenhagen). During this experiment, an approximately 700 km long profile along the Faeroe-Iceland ridge from the Faeroes to the Neovolcanic zone of Iceland was surveyed. In Iceland, the FIRE profile extended 170 km eastward from the western border of the Northern Volcanic Zone, to the Reydarfjördur fjord in eastern Iceland. This report is only concerned with the Krafla Undershooting Experiment, i.e., the part of the FIRE-profile that lay within the Neovolcanic zone. The undershooting experiment was carried out by the Lamont-Doherty Earth Observatory of Columbia University and the Science Institute of the University of Iceland.

A total of 38 seismic recorders from the PASSCAL/IRIS, LDEO, ICELAND and University of Nevada instrument pools was used in the undershooting experiment. Three configurations of instruments were used: 18 Reftek model 72A-06 recorders with Mark Products Model L22D geophones; 16 Scintrex model PRS-4 recorders with L22D geophones; and 4 Scintrex model PRS-4 recorders with Sprengnether (S-6000) 2 Hz geophones. The Reftek instruments recorded continuously at 50 samples/s and were timed by GPS-clocks. The PRS4 instruments recorded only timed

windows at 100 samples/s; their quartz crystal clocks were frequently synchronized using the MSF radio time signal from Rugby. All geophones were 3-component, with a response flat to ground velocity above their 2 Hz corner frequency. Further information about the general performance of L22-D geophones is given in Menke et al. [1991]. The traveltimes were hand picked from a computer screen, with an accuracy of ±0.01-0.02 s for first arrivals and ±0.02-0.03 s for later arrivals. When generating record sections, we discovered a systematic offset in arrival readings between the two types of instruments, which we compensated for by advancing the PRS-4 arrivals by 40 ms.

Seismic signals were generated by detonating explosives charges in lakes and around the coasts of northern and eastern Iceland. The charges were placed in lakes or in the ocean and were detonated by an electric pulse controlled by a Nanometrix model F-501 clock. The clock was synchronized to the MSF radio time signal from Rugby, usually within a few hours before and after each shot. All PRS4 recorders were synchronized to Rugby time at the beginning and end of each deployment, and also, if possible, during deployments (Appendix A). The shot times given in Table 1 have been corrected for the drift of the clock. A small delay is associated with the firing mechanism, estimated to be within 20 ms. The 1994 shots were recorded with one vertical 2 Hz geophone connected to a PRS4 digital recorder near the shotsite, usually within 300 m.

The locations of the shots and stations were determined by GPS navigation, using a Magellan Model NAV5000-PRO GPS receiver. Readings on water were made as close to the site as possible and averaged for as long as was practical given the currents and boat drift. The shot and station sites were located with a minimum radial accuracy of ± 30 m (Table 1).

Two perpendicular refraction profiles were surveyed across the Krafla central volcano. First, we surveyed a 20 km long NS-profile (Figure 4). Three shots were detonated on this profile, one to the north in Axarfjördur, one to the south in Askja, and one in center of the profile in the 1724 explosion crater Víti (Figure 1). Second, a 55 km long EW-profile, from Geitafell to Jökulsá á Fjöllum, was surveyed from 6 shotsites, two to the west (Eyjafjördur and Skjálfandi), three to the east (in Sænautavatn, Lögurinn and Reydarfjördur), and one within the profile at Víti (Figure 1). The 1994 profiles crossed the Krafla caldera in the same region as the 1993 reflection/refraction profiles (Figure 4). Both profiles had an average receiver spacing of 500 m within the Krafla caldera and 1-4 km elsewhere. Individual station locations from the different experiments are listed in Table 2.

TABLE 1: SHOTSITE LOCATIONS AND DATES, 1991, 1993, 1994.

Year	Day no.	Time (h m s)	P-arriv. Shot site	Latitude	Longitude	Water depth (m)	Charge (kg)	Location
1991								
08 10	222	08 00 00.224		66N 59.90	17W 42.10	341	100	E01
08 10	222	19 30 00.108		66N 15.294	16W 35.435	159	101.8	E35, Axarfjördur
08 10	222	22 29 59.858		66N 28.765	17W 32.964	294	101.8	E36
08 11	223	09 29 59.857		66N 22.667	17W 53.378	62	41.4	E37
08 11	223	11 59 59.330		66N 16.862	18W 14.569	138	43.2	E38
08 13	225	00 30 00.200		66N 43.067	16W 45.462	10	100	Víti, Krafla
1993								
04 09	099	23 30 00.000		66N 43.067	16W 45.462		10	Víti, Krafla
04 10	100	16 00 00.015		66N 43.067	16W 45.462	05	05	Víti, Krafla
04 10	100	17 00 00.017		66N 42.94	16W 48.03	12	10	Leirhnúkur
04 10	100	18 00 00.019		66N 44.262	16W 55.992			Gæsadalur
04 11	101	11 00 00.005		66N 43.067	16W 45.462	08	15	Víti, Krafla
04 11	101	12 00 00.006		66N 42.94	16W 48.03	12	15	Leirhnúkur
04 11	101	13 00 00.008		66N 44.262	16W 55.992		15	Gæsadalur
04 11	101	16 00 00.014		66N 44.262	16W 55.992		10	Gæsadalur
04 11	101	17 00 00.016		66N 42.94	16W 48.03	12	15	Leirhnúkur
04 11	101	19 00 00.019		66N 43.067	16W 45.462		30	Víti, Krafla
1994								
07 27	208	11 01 00.00	60.07	65N 43.067	16W 45.462	40	050	Víti, Krafla
07 28	209	11 01 00.00	60.08	65N 43.067	16W 45.462	40	7.2	Víti, Krafla
07 29	210	08 01 00.00	60.19	66N 16.774	16W 29.740	50	100	Axarfjördur
07 30	211	16 01 00.00	60.12	65N 02.597	16W 46.155	50	100	Askja
08 02	214	23 01 00.00	60.12	65N 00.993	14W 10.602	59	200	Reydarfjördur
08 03	215	14 01 00.00	60.11	65N 05.987	14W 45.260	50	150	Lögurinn
08 03	215	22:01:00.00	60.16	65N 16.668	15W 31.410	23	100	Sænautavatn*
08 04	216	14 01 00.00	60.09	65N 43.067	16W 45.462	40	093	Víti, Krafla
08 04	216	14 14		65N 43.067	16W 45.462	04	1.8	Víti, Krafla
08 05	217	22 01 00.00	60.25	66N 01.595	17W 38.543	54	200	Skjálfandi
08 06	218	20 01 04.00	60.19	65N 56.783	18W 15.373	64	200	Eyjafjördur

* obtained from map

TABLE 2a: STATION LOCATIONS, NS-profile, Krafla, 1994,

Sensor/ Station	Latitude		Longitude		Alt (m)	Map (m)	AVG (no)		Stand. Dev.	XPDOP
502/n16	65N	47.3126	16W	43.5237	450		POS	3D		
NE4/P15	65N	46.5333	16W	43.8643	497	500	(200)	3D	(22.5)	2.7
499/n15	65N	46.1928	16W	43.8821	550		POS	3D		
350/P14	65N	45.6818	16W	43.5845	648	615	(400)	3D	(26.4)	3.6
1501/n14	65N	45.4894	16W	43.6776	563		POS	3D		
516/P13	65N	45.31	16W	43.80	652	625	POS	3D		
1496/n13	65N	45.1957	16W	43.7215	738		POS	3D		
517/P12	65N	44.8691	16W	44.2766	634	630	(400)	3D	(37.3)	2.3
448/n12	65N	44.5545	16W	44.2816	751		POS	3D		
1505/gaes	65N	44.3793	16W	57.1709	305		POS	3D		
356/P11	65N	44.2045	16W	44.2441	600	620	(200)	3D	(45.0)	4.0
781/n11	65N	44.0373	16W	44.3673	668		POS	3D		
354/P10	65N	43.7863	16W	44.8519	686	575	POS	3D		
1486/n10	65N	43.6073	16W	45.1150	478		POS	3D		
353/P9	65N	43.4607	16W	45.3417	553	570	(500)	3D	(32.5)	4.6
502/holl	65N	43.4430	16W	52.9095	486		POS	3D		
437/n9	65N	43.2138	16W	45.2317	478		POS	3D		
351/P8	65N	43.0025	16W	45.6497	548	560	(500)	3D	(27.5)	4.6
501/leis	65N	43.0000	16W	47.4225	477		POS	3D		
359/P7	65N	42.8082	16W	45.4366	650	550		3D	(3.8)	3.2
465/n8	65N	42.6871	16W	46.1621	399		POS	3D		
352/PS	65N	42.27	16W	44.82		625		MAP		
473/obsi	65N	42.1467	16W	42.1526	547		POS	3D		
NE2/PG	65N	42.1276	16W	44.9743	550	600	(400)	2D	(23.2)	1.5
477/n7a	65N	42.0650	16W	46.8224	432		POS	3D		
477/n7	65N	42.0049	16W	46.7373	476		POS	3D		
358/P6	65N	41.70	16W	46.53		460		MAP		
440/n6	65N	41.4974	16W	46.0690	394		POS	3D		
357/P5	65N	41.0807	16W	46.1582	415	420	POS	2D		
500/n5	65N	40.7411	16W	46.5652	329		POS	3D		
NE3/P4	65N	40.4282	16W	47.0965	416	390	(400)	3D	(20.3)	2.3
NE1/P3	65N	39.998	16W	47.411	427	390	POS	3D		
1493/n4	65N	39.9333	16W	46.5534	380		POS	3D		
518/P2	65N	39.4719	16W	48.5546	460	440	(100)	3D	(9.8)	3.5
509/n3	65N	38.9487	16W	47.6494	419		POS	3D		
355/P1	65N	38.8688	16W	49.2273	421	425	(400)	3D	(31.0)	3.4
9360/PA	65N	38.3718	16W	49.3426	456	470	(400)	3D		
9337/PB	65N	38.0767	16W	48.7677	368	365	(400)	3D		
498/n2	65N	37.4875	16W	48.1956	359		POS	3D		
355/PC	65N	36.3145	16W	50.4330	414	360	(200)	3D	(13.3)	4.3
9337/PD	65N	35.7383	16W	50.5815	450	390		3D		3.0

n13 geophone N20°W; n12 geophone N5°; n11 geophone N90°W; n10 geophone N38°E
n8 geophone N18°E; n4 and n5 geophones N16°E; n2 and n3 geophones N11°E

TABLE 2b: STATION LOCATIONS, EW-profile, Krafla, 1994,

Sensor/ Station	Latitude		Longitude		Alt (m)	Map (m)	AVG (no)		Stand. Dev.	XPDOP
448/e158	65N	33.6421	16W	11.2211	335		POS	3D		
1486/e157	65N	36.5286	16W	14.3630	316		POS	3D		
1493/e156	65N	38.4828	16W	21.8793	335		POS	3D		
499/e155	65N	39.1600	16W	28.1793	390		POS	3D		
498/e153	65N	39.5361	16W	36.3713	434		POS	3D		
509/e152	65N	41.0975	16W	40.2436	537		POS	3D		
473/obsi	65N	42.1467	16W	42.1526	547		POS	3D		
440/e150	65N	42.0594	16W	43.6940	555		POS	3D		
357/HRH	65N	42.0686	16W	43.0375	684	650	(200)	3D	(25.1)	4.6
352/GIL	65N	42.2330	16W	44.0194	681	600		3D	(30.9)	4.1
518/H-18	65N	42.08	16W	44.21		610		MAP		
781/n11	65N	44.0373	16W	44.3673	668		POS	3D		
NE2/PG	65N	42.1276	16W	44.9743	550	600	(400)	2D	(23.2)	1.5
1496/n9	65N	43.2138	16W	45.2317	478		POS	3D		
9360/H-10	65N	42.7620	16W	46.0458	542	545	POS	3D		
465/n8	65N	42.6871	16W	46.1621	399		POS	3D		
477/n7b	65N	41.7669	16W	46.2718	351		POS	3D		
500/n5	65N	40.7411	16W	46.5652	329		POS	3D		
9337/V2	65N	42.79	16W	47.00		530		MAP		
501/leis	65N	43.0000	16W	47.4225	477		POS	3D		
NE4/V3	65N	42.75	16W	47.49		530		MAP		
356/L1	65N	43.0448	16W	48.0578	552	540		3D		3.2
351/L2	65N	43.0788	16W	48.4341	610	525	POS	3D		
359/L3	65N	43.1853	16W	48.9026	517	520		3D		2.4
451/e147	65N	42.6948	16W	49.2929	484		POS	3D		
355/L4	65N	43.2233	16W	49.4633	551	515		3D		3.6
350/L5	65N	43.3288	16W	49.9765	463	510		3D		5.7
NE3/HVA	65N	43.4516	16W	51.6251	509	500	(50)	3D		
(NE3/HVA	65N	43.4705	16W	51.6004	687	500	(50)	3D)		
502/holl	65N	43.4430	16W	52.095	486		POS	3D		
354/MUL	65N	43.9378	16W	53.5608	539	540	(50)	3D		
(353/TJA	65N	44.1311	16W	55.1271	381	515	(50)	3D)		
353/TJA	65N	44.0748	16W	55.0564	534	515		3D		
1505/gaes	65N	44.3793	16W	57.1709	305		POS	3D		
516/BOG	65N	44.8658	16W	59.7217	272	410	(200)	3D	(22.4)	3.8
NE1/BOH	65N	45.4913	17W	00.3349	447	400	(200)	3D	(22.5)	3.8
517/BON	65N	45.8890	17W	03.7080	354	400	(100)	3D	(19.6)	3.6
358/GEI	65N	47.6435	17W	15.5930	277		(200)	3D	(44.3)	3.1

n7b geophone was aligned N10°E; n8 geophone N18°E
n11 geophone N90°W; GEI geophone N20W

TABLE 2c: STATION LOCATIONS, Krafla, 1993,

Sensor/ Station	Latitude		Longitude		Alt (m)	Map (m)	AVG (no)	Stand. Dev.	XPDOP
vt1	65N	43.170	16W	45.590	565				
vt2	65N	43.100	16W	45.860	550				
vt3	65N	43.040	16W	46.090	545				
vt4	65N	43.000	16W	46.350	535				
vt5	65N	42.930	16W	46.490	535				
vt6	65N	42.880	16W	46.820	538				
vt7	65N	42.860	16W	47.040	535				
vt8	65N	42.840	16W	47.270	530				
vt9	65N	42.850	16W	47.560	530				
vt10	65N	42.870	16W	47.870	545				
vt11	65N	43.00	16W	48.03	540				
vt12	65N	43.07	16W	48.31	535				
vt13	65N	43.15	16W	48.54	535				
vt14	65N	43.18	16W	48.77	525				
vt15	65N	43.17	16W	49.04	525				
vt16	65N	43.18	16W	49.30	523				
vt17	65N	43.21	16W	49.58	520				
vt18	65N	43.24	16W	49.80	505				
vt19	65N	43.26	16W	50.02	505				
vt20	65N	43.30	16W	50.35	505				
vt21	65N	43.31	16W	50.56	505				
vt22	65N	43.37	16W	50.88	495				
vt23	65N	43.39	16W	51.06	495				
vt24	65N	43.36	16W	51.37	495				
vt25	65N	43.29	16W	51.57	490				
vt26	65N	43.21	16W	51.82	540				
vt27	65N	43.16	16W	51.97	540				
vt28	65N	43.06	16W	52.20	540				
vt29	65N	43.02	16W	52.43	540				
vt30	65N	42.98	16W	52.65	540				
vt31	65N	43.07	16W	52.83	545				
vt32	65N	43.15	16W	52.99	540				
vt33	65N	43.19	16W	53.25	550				
vt34	65N	43.16	16W	53.55	550				
vt35	65N	43.15	16W	53.92	550				
vt36	65N	43.10	16W	54.10	550				
vt37	65N	42.99	16W	54.57	530				
vt38	65N	42.93	16W	55.06	530				
vt39	65N	43.10	16W	55.58	520				
vt40	65N	43.25	16W	55.84	490				
vt41	65N	43.46	16W	56.14	500				
vt42	65N	43.59	16W	56.37	490				
vt43	65N	43.77	16W	56.74	490				

TABLE 2d: STATION LOCATIONS, Krafla, 1991.

Sensor/ Station	Latitude		Longitude		Alt (m)	Map (m)	AVG (no)	Stand. Dev.	XPDOP
gdl	65N	44.380	16W	57.079	440				
hva	65N	43.707	16W	51.464	500				
ytr	65N	42.711	16W	51.836	525				
nhl	65N	41.630	16W	53.512	500				
shl	65N	40.274	16W	52.449	420				
rey	65N	38.541	16W	53.570	300				
vog	65N	37.379	16W	54.829	280				
gyd	65N	36.262	16W	55.798	280				
hof	65N	34.961	16W	57.105	280				
gar	65N	33.716	16W	56.625	280				

2.2 The 1993 Krafla Reflection Survey

In April 1993, a reflection profiling study was conducted within the Krafla central volcano by scientists from the University of Bergen (Norway), the University of Iceland, and the National Energy Authority of Iceland. The objectives of this study were to define the shallow (<3 km) seismic structure above the region where Einarsson [1978] reported S wave shadows and, if possible, to map the surface of the Krafla magma chamber. As shown in Figure 4, two profiles were surveyed: a 4 km, unreversed NS profile, with two shots at the southern end, at Víti; and a 9 km, reversed EW profile across the caldera with repeated dynamite shots at the western end of the profile at Gæsadalur, at the eastern end at Víti, and within the profile at Leirhnúkur. The same PRS4/L22D instruments described above were used in this experiment. The two profiles had an average station spacing of 200 m. A 'Snowstreamer' seismic reflection array and two Vibroseis trucks were also used during this experiment. However, no reflection data are presented in this report.

2.3 The 1991 Tjörnes Fracture Zone (TFZ) experiment

We use data from a sideline of the Tjörnes Fracture Zone study [Sturkell et al., 1993] which was mainly concerned with the seismic structure along the north coast of Iceland. The sideline consisted of a single NNE-SSW line with 9 stations, located at an average interval of 2.5 km along the western part of the Krafla fault swarm (Figure 4). The Krafla array was deployed in order to search for Moho reflections and also to test the feasibility of a more ambitious undershooting experiment. The same PRS4/L22D instruments described above were used during this experiment. A single shot in Axarfjördur (labeled E35 by Sturkell et al., [1993]), about 65 km north of the profile, is used here.

2.4 General data reduction and analysis

The Krafla Power Plant served as a base-camp during the 1993 and 1994 experiments. Primary data reduction, carried out during the fieldwork, consisted of computer filing individual shots and earthquakes along with all relevant station, source, and timing information.

The seismic waveform data were all transcribed from their native format into LDEO AH format and the source and receiver information added to the AH headers. Timing errors and geophone misorientations were corrected at this stage and the waveform data were rotated into vertical, radial, and transverse components. At each processing stage, the data were plotted as record sections and carefully examined for evidence of errors.

Arrival times for all observed seismic phases were measured by eye from computer displays of the waveform data. The phase picks were superimposed on record sections and iteratively corrected and adjusted until correct. Bandpass filtering was occasionally used to improve the signal-to-noise ratio of the waveform data. However, the picks were always checked against the original seismograms to guard against timing errors introduced by the filtering process.

3 Upper structure of the Krafla caldera from seismic refraction

The uppermost 3 km within the Krafla caldera, including the roof of the magma chamber and high-temperature geothermal regions, were the focus of extensive seismic, geodetic, and geochemical monitoring surveys throughout the Krafla rifting episode. Various geodetic measurements (tilt and baseline measurements) were carried out in order to monitor changes in the caldera roof [Tryggvason, 1980; 1984; 1986] and extensive geochemical analyses undertaken to monitor the overall performance of the Krafla-Leirhnúkur geothermal system, including its magmatic contamination [Stefánsson, 1981; Óskarsson 1984; Ármannsson et al., 1987]. A triangular network of three seismic stations, established in 1974-1975 and expanded to 5 stations in the early 1980's, served as monitoring system of volcanic activity within the Krafla volcano. A one-dimensional crustal model, KRA73, derived from local refraction surveys conducted in 1971-1973 by the National Energy Authority has been used to locate seismic the activity within the Krafla volcanic system. The 1-D model was generated by fitting all available traveltimes and determining station correction coefficients from the varience at individual stations [Einarsson, 1978].

The 1993 and 1994 reflection/refraction surveys were the first high resolution experiments conducted within the Krafla caldera (Figure 4). The close (200 m)

station spacing and near-shot (100 m) station locations provide new information about the shallowest (<400 m) structure, which older experiments missed. Our 1993 profiles generally constrain the compressional wave velocity down to a depth of about 2 km as 10 km long raypaths turn at that depth, within the roof of the Krafla magma chamber.

The 1993 and 1994 data are organized into two profiles which cross the Krafla caldera at the Víti shotsite. The EW profile crosses both of Einarsson's [1978] shear wave attenuation zones, as well as the inflation/deflation center, which was active during the Krafla rifting episode [Tryggvason, 1980]. The NS profile traverses the eastern shear wave attenuation zone. Both profiles overlap the Leirbotnar-Sudurhlídar and Leirbotnar-Hvíthólar well fields (Figure 5) [Ármannsson et al., 1987] and extend well beyond the caldera rims. The borehole cross sections provide fundamental information about the lithology of the uppermost 2200 m along a 2 km long section of the EW profile just east of Víti (Figure 5a) and a 3 km long section of the NS profile south of Víti (Figure 5b).

The Krafla geothermal field is divided into two zones: An upper, water-dominated system with a mean temperature of 205°at 200-1100 m depth and a lower, boiling system with 300-350°temperatures [Stefánsson, 1981]. The geology of the Krafla well field can be divided into two main sequences: An upper, extrusive section and a lower, intrusive section. The upper part, dominated by alternating hyaloclastite and basaltic units, is 900-1500 m thick and is underlain by basaltic intrusives [Ármannsson et al., 1987]. The intrusives have a thickness of 900-1100 m in the Sudurhlídar field. Geological cross sections compiled from boreholes in other geothermal areas in Iceland show that the subsurface lithology in the uppermost 1000-2000 m to be dominated by alternating basaltic lavas and hyaloclastites, in variable proportions. The lithology of the Krafla cross sections reflects the geomorphology of the Neovolcanic zone in general, which is characterized by table mountains, hyaloclastite ridges, and postglacial lava fields.

The Víti shotsite is located 700 m from boreholes 4 and 10 in the Leirbotnar-Sudurhlídar well field and 1200 m from borehole 11 (Figure 5). Borehole drill cuttings show that the uppermost 900-1100 m in that region are made up of extrusives, i.e., alternating basaltic lavas and hyaloclastites which Ármannsson et al., [1987] divide into three major formations (M-1, B-2, and M-2). The uppermost sequence consist of a 200-300 m thick hyaloclastite unit (M-1) overlying a 200-300 m thick basaltic sequence (B-2) and a 350 m thick hyaloclastite sucession (M-2). The silicic tephra apron from the May 1724 explosion in Víti lies at the surface around the shotsite.

The observed traveltimes along the reversed 1993 EW-profile (Figure 6a) from the Gæsadalur and Víti shotsites are almost identical, which indicates that no major lateral heterogeneities exits in the uppermost crust within the caldera, i.e., no signif-

TABLE 4: CRUSTAL MODELS

1973-model		1993-model		EW-1995		GP-Icel. 1963		KATLA-94	
depth (km)	P-vel. (km/s)	depth (km)	P-vel. (km/s)	depth (km)	P-vel. (km/s)	depth (km)	P-vel. (km/s)	depth (km)	P-vel. (km/s)
0.0	2.4	0.0	1.1	0.00	1.20	0.0	2.8 (0)	0.00	3.30
0.5	3.8	0.1	2.0	0.26	2.67	0.7	4.2 (1)	0.50	4.00
2.5	5.2	0.2	3.0	0.60	4.10	2.0	5.1 (2)	1.50	5.00
5.0	6.5	1.0	4.5	0.80	4.84	3.65	6.3 (3)	4.50	6.00
		2.0	5.5	1.00	5.40				
		5.0	6.5	1.24	5.93				
				1.28	3.07				
				1.44	2.98				
				1.48	6.16				
				1.60	6.27				
				1.65	3.00				
				1.78	3.02				
				1.82	6.33				
				2.59	6.46				

icant dipping layer boundaries or large velocity anomalies occur at less than 2 km depth. However, small, local deviations from the average (calculated) traveltime curve occur. One such deviation appears 2.5 km east of the Gæsadalur shotpoint (filled circles in Figure 6a), where the P wave is advanced 0.1 s relative to the reversed profile. This anomaly is most likely caused by higher velocity material (intrusives) within the caldera than at comparable depths outside of it. Small, (0.1 s) systematic traveltime differences are also observed along the profiles. For instance, traveltimes south of Víti, on raypaths parallel to the Krafla fault swarm (filled circles in Figure 6b) are about 12% faster than those west of Víti, i.e., along raypaths perpendicular to the fault swarm.

Extremely low apparent P-wave velocities of about 1.1 km/s are observed adjacent to the shotsites. The uppermost raypaths from the Víti shotsite travel through a fumarole field and the Víti 1724 tephra layer, whereas rays from Gæsadalur go through postglacial, basaltic lava flows. The Víti tephra is over 100 m thick next to Víti [Sæmundsson, 1991] but thins rapidly to about 1 m at a distance of 1 km, north and west of Víti. The extremely low P-velocity is thus associated with the unconsolidated tephra and porous recent lava flows adjacent to the shotsites. Elsewhere in Iceland, near-surface compressional velocities range from 1.6-2.0 km/s in the Neovolcanic zones, increasing progressively with age, to 3.0-4.7 km/s in the Tertiary regions [Flóvenz and Gunnarsson, 1991]. Thus, it cannot be considered abnormal to find P-wave velocites as low as 1.1 km/s in surface layers within central volcanoes.

We first constructed a 1-D regional model, KRA93, which provided an overall

fit to the traveltime data (Figure 7, Table 4). We used the subroutine TTGEN from the earthquake location program HYPOINVERSE [Klein, 1978] to calculate traveltimes. The KRA93-model fits the data considerably better than the older, KRA73-model, with one exception. The older model has a better fit to the 1994, NS-line data at ranges less than 6 km in Hlíðardalur, south of Víti (Figure 6). However, both 1-D models provide very low-resolution representation of the crustal structure. A detailed examination of the record sections reveal fine-scale velocity fluctuations which are presented below.

Two P-wave shadow zones are evident on the EW profile, within the Krafla caldera. They occur at a range of 3.0 km and 5.0 km from the Víti shotsite (Figure 8). The upper shadow zone is visible on all three record sections but the lower shadow zone is not visible from the central (Leirhnúkur) shotpoint, which has poor signal-to-noise ratios at these ranges. The shadow zones are caused by two, thin, approximately flat-lying, low-velocity layers that occur at a depth of about 1300 and 1700 m (bold curve in Figure 7, EW-model in Table 4). The vertical traveltime of 0.08-0.10s through these low-velocity layers is tightly constrained by the traveltime offset. Their thickness trades off with velocity to some degree. Our best fit gives a thickness of 240 m for the shallower layer, with a compressional velocity of 3.0 km/s. Thicknesses greater than 375 m (with a velocity of 4.2 km/s) result in unacceptably little overlap in the traveltime branches. Therefore, a thickness of 375m should be considered as an upper bound. The lower layer has similar characteristics. The compressional velocity, just above and below the low velocity layers, ranges from 5.9-6.3 km/s.

The upper shadow zone is clearly absent on the NS profile, north of Víti. Although no lower seated shadow zones are detected elsewhere along the NS profile, either, the station spacing along that profile is probably too coarse to completely rule them out. In any case, observed differences between the two profiles indicate some degree of lateral heterogenity, in the uppermost 2 km within the Krafla caldera.

In order to improve the resolution of the shallow caldera structures, we created two-dimensional, NS (Figure 9) and EW (Figure 10) velocity models, using the Caress et al. [1992] RTMOD forward modelling program and a iterative, trial-and-error approach. The compressional velocity is represented in the model by continuous linear splines on a triangular mesh. We iteratively perturbed a starting, 1-D model until we are able to fit the small traveltime anomalies (Figure 11). The ray coverage, which is derived from three shotpoints on the EW profile but only a single shot on the NS profile, is not sufficient to uniquely determine the two dimensional structure. We can only claim that our final models give a general sense of the locations and amplitudes of the lateral heterogeneities.

Two main features appear on our caldera profiles: 1) Pálmason's [1963, 1971] Layer 3 (isovelocity surface 6.5 km/s) ascends beneath the caldera, where is reaches

a minimum depth of 1.6 km and; 2) Two low-velocity zones, observed along the EW-profile sit above the high-velocity dome. The minimum depth (1.6 km) of Layer P-3 which we observe beneath Krafla is 2 km less than Pálmason's [1963] estimate. Comparing our 2-D, crustal model of the Krafla caldera to the regional (Mývatn) crustal structure [Pálmason, 1963] (Table 4) we find that our depth to the 6.3 km/s isovelocity surface is also considerably shallower than the >4.5 km depth which Gudmundsson et al. [1994] observed beneath the Katla caldera in S-Iceland. However, it is not odd to find Layer P-3 at a shallower depth within central volcanoes [Pálmason, 1971; Flóvenz, 1980], which could explain the different observations in the Mývatn region. The Katla volcano is situated in the propagating (non-rifting) part of the EVZ. The Layer P-2 thickness is exceptionally high in that region with the Layer P2/P-3 boundary at a depth of 7 [Pálmason, 1971] to 9 km [Flóvenz and Gunnarsson, 1991]. The crustal structure of Gudmundsson et al's [1994] off-rift volcano is therefore not directly comparable to the structure of the Krafla rift zone volcano.

Pálmason's [1971] data showed that the shallowest depth to Layer P-3 is associated with volcanic centers which appear as local high-velocity anomalies (domes) in an otherwise layered crust. Flóvenz [1980], reinterpreting Pálmason's data, reported much higher linear velocity-depth gradients within the central volcanoes and estimated the depth to the Layer P-2/P-3 boundary could be as little as 1 km. Flóvenz [1980] called the central volcanoes, referring to their high-velocity doming, "chimneys through the Icelandic crust". He associated them with Pálmason's Layer 3 which he equated to Layer 3 in the oceanic crust. Others, associated Layer P-3 with metamorphic facies of basaltic rocks [Pálmason, 1971], and low-porosity basalts with high contents of epidote [Christensen and Wilkins, 1982; Flóvenz and Gunnarsson, 1991] instead of a heterogeneous mixture of basaltic intrusives and extrusives as [Bödvarsson and Walker, 1964] or sheeted dike complex [Walker; 1975]. Walker's [1975] interpretation of the nature of Layer P-3, being made up of intense regional swarm of intrusive sheets, is consistent with its Oceanic counterpart, which has been interpreted to consist of dikes (Layer 2C, V_p=6.1 km/s) and intrusive gabbros (Layer 3A, V_p=6.8 km/s) [Harrison and Bonatti, 1981; White et al., 1992]. The composition of Oceanic Layer 2C has been confirmed by drilling. Although the IRDP-hole in Reydarfjördur did not penetrate Layer P-3, it penetrated a number of dikes with a mean compressional velocity of 6.02±0.26 km/s, whereas the lava flows had a mean compressional velocity of 5.67±0.65 km/s [Christensen and Wilkins, 1982]. The dike intensity in the IRDP-hole varied between 31 and 44% [Robinson et al., 1982]. Our dense refraction profile and the lithological cross sections of the Krafla geothermal fields confirm that Bödvarsson and Walker's [1964] interpretation of the composition of Layer 3 was correct. A P-velocity of 6.25 km/s has to be associated with basaltic intrusives (dikes) at shallow depths within a

central volcano. However, outside the central volcanoes, the Layer 3 velocity can be ascribed to all the above mentioned, compositional variations.

The 1300 and 1700 m deep low velocity zones are not associated with shear wave shadow zones and therefore cannot represent layers of melt. Indeed, the traveltime of the S wave, which is clearly present from the Gæsadalur shotpoint, tracks that of the P wave very closely, with V_p/V_s=1.76 (Figure 12). Thus, the very low velocity is probably due to high porosities. Wyllie et al's [1958] formula, which is a good fit to measurements from Tertiary rocks at Reydarfjördur [Christensen and Wilkens, 1982], can be used to estimate porosity if the compressional velocity of the rock matrix is known. Using a matrix velocity appropriate for basaltic intrusives (6.25 km/s) and a fluid velocity appropriate for liquid water (1.5 km/s), we infer a porosity of 15-34% within the low velocity layer. However, Stefánsson [1981] argues that the steam fraction in the lower zone of the Krafla geothermal field is 10-20%, an effect which would lower our porosity estimates to 12-27%. The estimated porosity in the 200-1100 m deep, upper zone of the Krafla geothermal field is 15% [Stefánsson, 1981] and the average porosity measured in the Reydarfjördur borehole is 9% [Jónsson and Stefánsson, 1982]. The main aquifers of the Leirbotnar geothermal field follow hyaloclastite/basalt boundaries at 400 and 800 m depth and the upper boundary of a granophyre intrusion at 1900-2100 m depth. The main aquifers of the Sudurhlídar system are connected to lateral, acid intrusions at 900-1200 m depth [Ármannsson et al., 1987]. Hence, it is plausible that the low velocity layers we observe at 1300 and 1700 m depth are associated with similar high-porosity, geothermal aquifers.

3.1 Comparison to Arnott and Foulger's model of Krafla

Our model of the compressional velocity structure in the uppermost 2 km of the Krafla caldera differs in two fundamental ways from the model proposed by Arnott and Foulger [1994a]. Their model has much higher near-surface velocities and is more laterally heterogeneous than ours. Neither of these features are observed in our data (Figure 11, dotted lines). Their model predicts traveltimes that are as much as 0.3 s lower than we observe. Their predicted traveltime curves generate much stronger, small-wavelength traveltime anomalies than we observe, e.g., the anomaly they predict at the western caldera rim (their Figure 7b), at a distance of 7-8 km on Figure 11C. Arnott and Foulger [1994a] do not discuss how velocity, depth of hypocenters, and origin time of earthquakes trade off in their inversion process. We find no way of reconciling their model with the observed traveltime data. Therefore, we conclude that their model is, unfortunately, seriously flawed.

We believe that the flaw is related to their underlying methodology, which is based on arrival time data from local microearthquakes, and which employs a

simultaneous inversion for hypocentral parameters and velocity structure. Given optimum ray coverage such an inversion can indeed determine both the location and origin time of earthquakes and the three-dimensional velocity structure of the earth. Unfortunately, the spatial distribution of earthquakes in their dataset which are mainly confined to the caldera center (near Leirhnúkur), is far from optimum. Under such circumstances, velocity structure can trade off with the hypocentral depth and origin time.

This effect can be understood by considering how arrival time data are used to distinguish a deep earthquake from a shallow one. If the earth is laterally homogeneous (e.g., as at a distance of 0 to 10 km in Figure 13), then the traveltime curves from these two earthquakes differ in two ways: 1) The deeper earthquake has faster apparent velocities at short ranges; and 2) The deeper earthquake has longer traveltimes. Note, however, that the difference in traveltime is meaningful only when the origin time of the earthquakes is accurately known. If the earth is made laterally heterogeneous, with the velocity increasing with distance from the hypocenter, then the apparent velocities of the two traveltime curves become much more similar (as at a distance of 10 to 20 km in Figure 13). The difference in traveltime remains, but it can be traded off with origin time to produce identical arrival times. Thus, in our example, a 3 km deep earthquake in a laterally homogeneous earth has the same arrival time as a 1.5 km deep earthquake in a laterally heterogeneous earth (Figure 14). If widely separated hypocenters were available, then the ambiguity could be resolved, since one cannot make the velocity increase with distance from all the earthquakes simultaneously. But if they are clustered in one region, velocity can trade off with hypocenter depth.

Another point to consider is that Arnott and Foulger's [1994a] high-velocity anomalies at shallow depth will generate Bouguer gravity anomalies close to 10 mGals, using the velocity-density relationship from Christensen and Wilkens [1982], wheras the anomalies observed in the Krafla region do not exceed 5 mGals [Karlsdóttir et al., 1978], (Arnott and Foulger [1994a], Figures 3 and 7, and plate 1). As we discussed earlier, borehole cross sections show that two fairly uniform crustal sections exist within the Krafla caldera, above 2 km depth and that gabbroic intrusives are only found below 2000 m depth [Ármannsson et al., 1987].

Therefore, we believe that the high velocity anomalies that Arnott and Foulger [1994a] propose for the caldera rims, as well as their shallow (1-2 km) hypocentral depths, are artifacts of their inversion methodology.